Atmospheric Environment 89 (2014) 749–756

Contents lists available at ScienceDirect

Atmospheric Environment

journal homepage: www.elsevier.com/locate/atmosenv

# Gas-phase reactive nitrogen near Grand Teton National Park: Impacts of transport, anthropogenic emissions, and biomass burning

A.J. Prenni [a,*], E.J.T. Levin [a], K.B. Benedict [a,1], A.P. Sullivan [a], M.I. Schurman [a], K.A. Gebhart [b,c], D.E. Day [c], C.M. Carrico [d], W.C. Malm [c], B.A. Schichtel [b,c], J.L. Collett Jr. [a], S.M. Kreidenweis [a]

[a] Department of Atmospheric Science, Colorado State University, Campus Delivery 1371, Fort Collins, CO 80523, USA
[b] National Park Service, Fort Collins, CO, USA
[c] Cooperative Institute for Research in the Atmosphere, Fort Collins, CO, USA
[d] AECOM, 1601 Prospect Parkway, Fort Collins, CO 80525, USA

## HIGHLIGHTS

- Gas phase reactive nitrogen species were measured near Grand Teton National Park.
- A diel cycle was observed in ambient reactive nitrogen concentrations.
- Ambient concentrations were driven, in part, by mountain-valley circulation.
- Biomass burning resulted in elevated concentrations of reactive nitrogen.

## ARTICLE INFO

*Article history:*
Received 20 August 2013
Received in revised form
5 March 2014
Accepted 8 March 2014
Available online 12 March 2014

*Keywords:*
Grand Teton National Park
Reactive nitrogen
Biomass burning
Ammonia
$NO_x$
$NO_y$

## ABSTRACT

Excess inputs of reactive nitrogen can adversely affect terrestrial and aquatic ecosystems, particularly in sensitive ecosystems found at high elevations. Grand Teton National Park is home to such sensitive natural areas and is in proximity to potentially large reactive nitrogen sources. The Grand Teton Reactive Nitrogen Deposition Study (GrandTReNDS) was conducted in spring–summer 2011, with the aim of better understanding sources of reactive nitrogen influencing the region, spatial and temporal variability of reactive nitrogen in the atmosphere, and current levels of nitrogen deposition. Overall, $NO_y$ was determined to be the most abundant class of ambient gas phase reactive nitrogen compounds, and ammonia was determined to be the most abundant individual nitrogen species. $NO_x$, $NO_y$ and $NH_3$ concentrations all showed a diel cycle, with maximum concentrations during the day and minimum concentrations at night. This pattern appeared to be driven, in part, by mountain-valley circulation as well as long range transport, which brought air to the site from anthropogenic sources in the Snake River Valley and northern Utah. In addition to the nitrogen sources noted above, we found elevated concentrations of all measured nitrogen species during periods impacted by biomass burning.

Published by Elsevier Ltd.

## 1. Introduction

Nitrogen emissions and deposition have been increasing in the western US (Fenn et al., 2003b), with increases in deposition especially evident at high elevations (Burns, 2003). Increased emissions are driven by anthropogenic sources, which have impacted even remote regions in the northern hemisphere since the beginning of the 20th century (Holtgrieve et al., 2011). Although large areas in the western US are exposed to low levels of atmospheric deposition (Fenn et al., 2003a), increases are sufficient to be detected and likely impact the biosphere at the hemispheric scale (Holtgrieve et al., 2011). Effects of excess nitrogen inputs are extensive, including impacts on water quality and nutrient cycling, nitrogen enrichment in soils and plants, eutrophication of lakes, decreased diversity of mycorrhizal communities, altered plant community composition, and impacts on drought, frost and pest tolerance (Bowman et al., 2006; Fenn et al., 2003a; Krupa, 2003). Ecosystems in the Rocky Mountains appear to be particularly sensitive to small increases in nitrogen (Bowman et al., 1993), where in some high elevation watersheds there has already been a shift from

*Abbreviations:* HTC-RN, high temperature conversion reactive nitrogen.

* Corresponding author.
*E-mail address:* anthony.prenni@colostate.edu (A.J. Prenni).

[1] Now at U.C., Davis, Davis, CA, USA.

http://dx.doi.org/10.1016/j.atmosenv.2014.03.017
1352-2310/Published by Elsevier Ltd.

nitrogen limited systems to ecosystems which are nitrogen saturated (Williams et al., 1996).

Reactive nitrogen sources are dominated by $NO_x$ ($NO + NO_2$) and ammonia ($NH_3$) (Galloway et al., 2004). In the atmosphere, $NO_x$ is typically converted to other $NO_y$ species ($NO_x$ plus other reactive oxidized nitrogen) such as $HNO_3$ in less than 1 day (Seinfeld and Pandis, 1998), which can then go on to influence the acidity of precipitation. There is substantial spatial and temporal variability in $NO_x$ concentrations, which range from sub-ppb levels in remote environments to more than 100 ppb in urban areas (Seinfeld and Pandis, 1998). For ammonia, more than 80% of emissions are from agriculture in the U.S. (Reis et al., 2009), primarily from livestock wastes and volatilization of $NH_3$-based fertilizers, while biomass burning serves as an important natural source (Kopacek and Posch, 2011). Ammonia emissions in the US increased ~20% between 1990 and 2005 (Reis et al., 2009), and global emissions are expected to continue to rise (Galloway et al., 2004).

Although many studies have focused on wet nitrogen deposition, dry deposition of ammonia is also an important deposition pathway in the Rocky Mountains (Beem et al., 2010; Benedict et al., 2013a, 2013b; Burns, 2003; Day et al., 2012), particularly because it has been shown to drive plant species change faster than wet deposition of ammonium (Sheppard et al., 2011). Dry deposition of ammonia is most important close to the source (Asman et al., 1998), resulting in large spatial variability, with concentrations ranging from sub-ppb levels in remote environments (e.g. (Alkezweeny et al., 1986)) to hundreds of ppb near agricultural sources (e.g. (Sintermann et al., 2011)). Re-emission of deposited ammonia via bi-directional exchange with plant surfaces (Massad et al., 2010) can potentially expand the spatial extent of these emissions. There is also seasonal variability, with atmospheric $NH_3$ concentrations typically peaking in spring and summer (Krupa, 2003).

Satellite measurements have identified the Snake River Valley in Idaho as a U.S. hotspot for ammonia emissions (Clarisse et al., 2009), and modeling results suggest that areas near the border of WY and ID, on the western side of Grand Teton National Park (GRTE), are likely to have extensive nitrogen deposition (Fenn et al., 2003b). While agricultural areas may thrive on the enriched nitrogen, natural vegetation is more sensitive to $NH_3$ inputs (Krupa, 2003), and high elevation lakes within GRTE have been identified as being particularly sensitive to inputs of inorganic nitrogen (Nanus et al., 2009). The Greater Yellowstone Ecosystem, which includes GRTE, has already shown signs of changes triggered by increased nitrogen inputs (Saros et al., 2011). In this paper, we report atmospheric concentrations of several gas phase nitrogen species at a high elevation site near GRTE in spring-summer 2011, as part of the Grand Teton Reactive Nitrogen Deposition Study (GrandTReNDS).

## 2. Material and methods

The core measurement site for GrandTReNDS was located ~6 km from the west boundary of GRTE (Fig. 1 inset), on Peaked Mountain at Grand Targhee Resort (latitude 43.78 N; longitude 110.94 W; elevation 2722 m). The vegetative environment at Grand Targhee Resort is subalpine. The measurement site was located at the transition zone between forest and the tree line, with Douglas-fir, subalpine fir, Whitebark pine and Engelmann spruce being the dominant vegetation in the immediate vicinity, and stands of other species such as lodgepole pine and aspen being present within a few miles of the site. Real time measurements at the core site began August 1 and continued through September 22, 2011. Measurements were carried out in the National Park Service (NPS) mobile air sampling laboratory. The laboratory is temperature-controlled (~25 °C) and includes space and power for instrumentation.

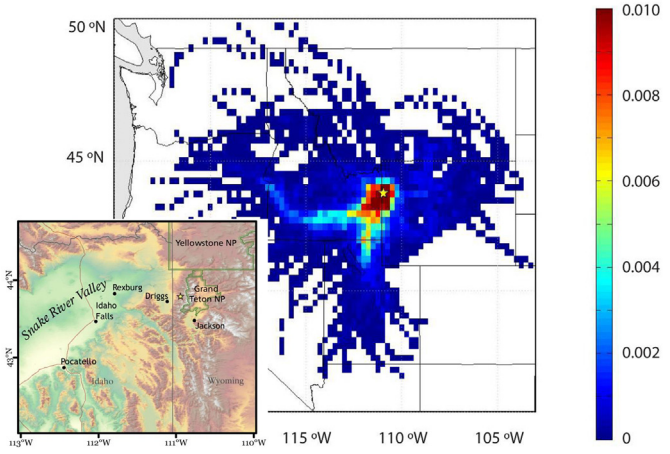


**Fig. 1.** Results from HYSPLIT 48 h back trajectory analysis for August 1, 2011–September 22, 2011. The location of the core site is shown as a star. Colors represent the fraction of time that a back-trajectory passed through a 0.2° × 0.2° grid box. Inset shows regional topography for area surrounding the sampling site. (For interpretation of the references to color in this figure legend, the reader is referred to the web version of this article.)

Back-trajectory residence time analysis using the Hybrid Single-Particle Lagrangian Integrated Trajectory model (HYSPLIT4) (Draxler, 1999; Draxler and Hess, 1998) with input from the NAM-12 meteorological data set provides insight regarding transport pathways of air masses impacting the site. Forty eight hour back trajectories initialized at 100 m AGL were run for every hour of the study period (August 1–September 22). Results from the study period show that the air masses came predominantly from the west, in the Snake River Valley, and the southwest, from northern Utah (Fig. 1).

### 2.1. Continuous gas measurements

Continuous gas measurements included ammonia ($NH_3$), $NO_x$, $NO_y$, carbon monoxide (CO), and an additional reactive nitrogen component described below. A schematic of the sampling strategy is summarized in Fig. 2. For $NH_3$, $NO_x$, CO and the additional reactive nitrogen component, sampling was from a common inlet ~3 m above ground level. The sampling line was ~1 m, 0.64 cm OD Teflon for $NO_x$, CO, $NH_3$ from the Air Sentry II Ion Mobility Spectrometer (IMS; Particle Measuring Systems), and the additional reactive nitrogen component. For these instruments, sample line residence time was <1 s. An additional ~1 m of sampling line was needed for $NH_3$ measured with a Picarro cavity ring down spectroscopy (CRDS) instrument; for the CRDS, residence time was ~2.5 s. This inlet included a PTFE filter with PFA housing (Mykrolis WGFG21KP3) upstream to remove particles. For $NO_y$, ambient air was sampled through a 6 m long, 0.64 cm OD Teflon sampling line, with an inlet ~2 m above ground level. Residence time in the sampling line was ~5 s. Calibrations for all instruments were performed prior to the study. All calibrations were done using certified, traceable standards provided by Airgas. Calibration gases were diluted using a Teledyne Zero Air Generator (Model 701) and Dynamic Dilution Calibrator (DDC, Teledyne Model 700). Every calibration included zero air and a span concentration, with calibration gases introduced at the sample inlets. For ammonia, sufficient time was allowed to ensure the calibration system was conditioned with ammonia (overnight). A separate line was added near the sample inlet to allow for collection and analysis of the calibration gas ($NH_3$) using a denuder. This method was used to account for any losses in the calibration system. For CO, $NO_x$, $NO_y$

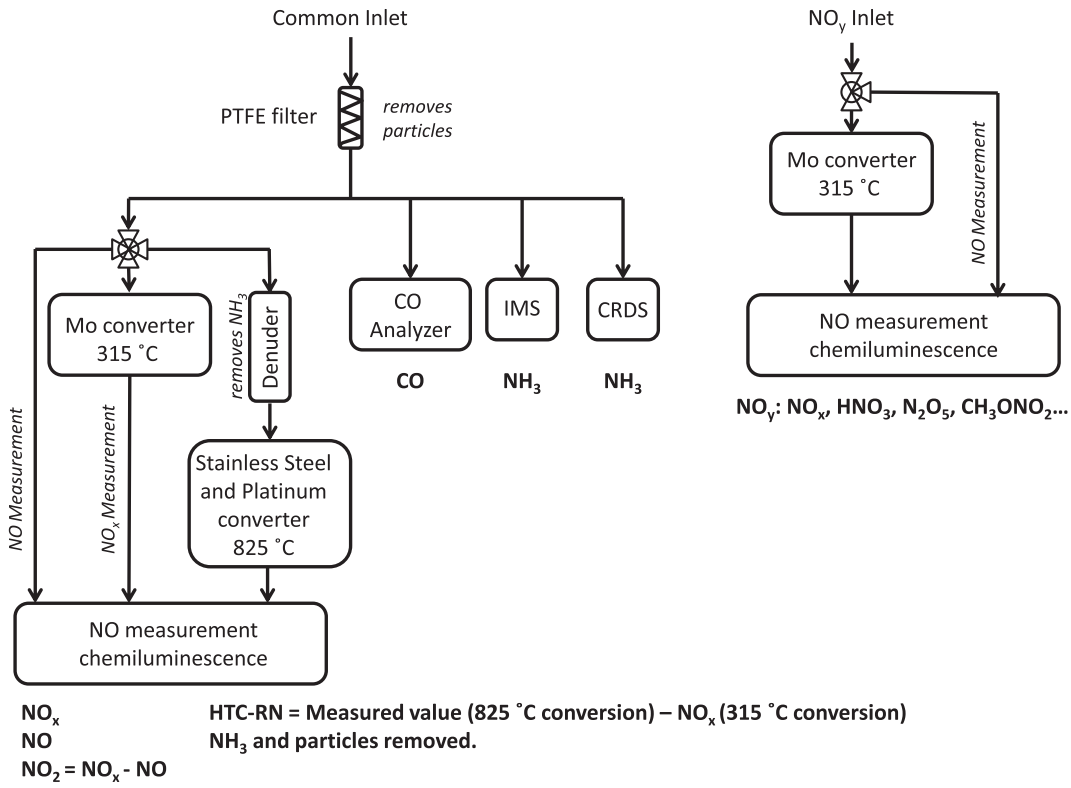


**Fig. 2.** Schematic of sampling setup.

and the additional reactive nitrogen measurement, four calibrations were completed between August 2 and August 26, after which calibrations were performed on an almost daily basis. Fewer calibrations were done early in the study due to a failing DDC; this unit was replaced on August 25. An intercomparison of redundant NO measurements from two instruments (described below) suggest that the $NO_y$ data collected August 18–August 25 may have been impacted by a calibration using the failing DDC. However, no clear deviations were observed in the $NO_y$ data during this time. For $NH_3$, additional calibrations were done approximately every 10 days.

Measurements of $NO_x$, NO and $NO_2$ were made using a chemiluminescence instrument (Teledyne 201E). The technique alternately measures nitric oxide (NO) directly and measures $NO_x$ by first converting $NO_2$ to NO using a molybdenum converter (315 °C) (Fehsenfeld et al., 1987; Parrish and Fehsenfeld, 2000). In this instrument and the $NO_y$ instrument described below there is a sufficient wait time between each measurement to ensure that the system is flushed with new sample air, so that there are no transients due to the valve switching. NO then is reacted with ozone forming $NO_2$ in an excited state which emits radiation while decaying to the ground state (Fontijn et al., 1970). $NO_x$ measurements via chemiluminescence likely also measure some $NO_y$ compounds other than NO and $NO_2$, as the conversion is nonspecific to $NO_2$ (Dunlea et al., 2007; Parrish and Fehsenfeld, 2000).

Measurements of $NO_y$ were made using a similar chemiluminescence instrument (Teledyne 200EU). As with $NO_x$, NO is measured directly and other $NO_y$ species are converted to NO using a molybdenum converter (315 °C). The primary differences between the $NO_y$ and $NO_x$ measurements are that the converter for the $NO_y$ instrument is located at the inlet to minimize losses, primarily of $HNO_3$, and the $NO_y$ sample does not pass through a filter before conversion. In addition to $NO_x$, the $NO_y$ instrument is thought to measure species including, but not limited to, $NO_3$, $HNO_3$, $N_2O_5$, $CH_3ONO_2$, $CH_3CH_2ONO_2$, n-$C_3H_7ONO_2$, n-$C_4H_9ONO_2$, and $CH_3CHONO$ (Dunlea et al., 2007). Particulate nitrate, HONO, $HO_2NO_2$, and $RO_2NO_2$ are also measured, although less effectively (Dunlea et al., 2007).

An additional reactive nitrogen component was determined using chemiluminescence (Teledyne 201E). For this measurement, ambient air passed through the PTFE filter and then passed through a URG annular denuder coated with 10% (w/v) phosphorous acid solution to remove ammonia, amines (Kallinger and Niessner, 1999), and any other rapidly diffusing basic species that react with the acid coating. This denuded sample was sent to a stainless steel and platinum converter heated to 825 °C (Teledyne 501NH). This high temperature catalyst allows for conversion of additional nitrogen species that were not converted at 315 °C, and when used without a filter or denuder provides a measure of total reactive nitrogen. This system is similar in principle to the Total Reactive Atmospheric Nitrogen Converter (TRANC) with fast response chemiluminescence detector (Marx et al., 2012), although the TRANC technique provides faster response measurements and quantitatively measures particulate nitrogen. For the measurements in this study the $NO_x$ concentration is then subtracted from the total measurement. Because the 825 °C converter and the $NO_x$ measurement are on the same inlet and sampling line, by subtracting the measured $NO_x$ concentration we effectively subtract any nitrogen compounds present that can be converted at 315 °C. Typically, this method is used to measure ammonia. In this study, however, ammonia and amines were removed, so that the measurement is presumed to be gas phase nitrogen species other than ammonia and amines which are converted at high temperature, but not at 315 °C. Collectively, we designate these compounds as high temperature conversion reactive nitrogen (HTC-RN). This measurement likely contains a variety of reduced organic nitrogen compounds; however, due to the lack of selectivity of the

measurement, other compounds may also be present, possibly including interferents from some VOCs that do not include nitrogen. Although the measurements are not quantitative, we include these observations as a measure of reactive nitrogen species which are not accounted for using standard techniques.

A trace level CO analyzer (Teledyne 300EU) served as a combustion tracer. The model 300EU is based on absorption of infrared radiation and has a detection limit of <20 ppb.

Two $NH_3$ measurements were employed: an Air Sentry II IMS and a Picarro CRDS. In the IMS (Hill et al., 1990), the sample is mixed with an ionization control reagent before ionizing the sample with a $^{63}Ni$ beta-emitting ionization source. A shutter grid is pulsed periodically to allow the analyte into the drift tube, where the ions accelerate in response to an applied electric field until they are ultimately detected at a collector plate. Measured ion time of flight is used for speciation and peak height for quantification. Although the IMS is meant to measure ammonia, amines also are detected.

The Picarro G1103 Analyzer for ammonia utilizes time-based, optical absorption spectroscopy. The instrument employs wavelength-scanned CRDS, in which a pulse of near infrared light passes back and forth between two mirrors in the presence of the ambient sample. A small fraction of this light leaks through one of the mirrors, where its intensity is monitored. A wavelength monitor is employed to ensure that only the spectral feature of interest is being monitored, in this case ammonia, and a water vapor correction is done in real time. The CRDS has weak sensitivity to some amines, which is not expected to impact the results. The rate of decay of light intensity is proportional to the ammonia concentration (Paldus and Kachanov, 2005).

### 2.2. Supporting measurements

During GrandTReNDS, aerosol number size distributions were measured over the diameter range 0.04–20 μm using a differential mobility particle sizer (TSI 3085), an optical particle counter (LASAIR 1003) and an aerodynamic particle sizer (TSI 3021). Measurements were combined to produce one continuous size distribution (Hand and Kreidenweis, 2002) with 15 min resolution. This integrated size distribution was used as a measure of condensation nuclei, although it does not include particles <40 nm. As such, it is designated $CN_{>40\ nm}$.

Daily hi-volume quartz filter samples were collected at a nominal flowrate of 1.13 $m^3\ min^{-1}$ through a two-filter assembly to separate particles with aerodynamic diameters greater than and less than 2.5 μm. An impactor in combination with a slotted filter collects particles greater than $PM_{2.5}$, followed by a 20.3 cm × 25.4 cm filter to collect $PM_{2.5}$. The $PM_{2.5}$ samples were extracted and analyzed for water-soluble potassium (Sullivan et al., 2011), organic carbon and elemental carbon (Birch and Cary, 1996).

Meteorological data were collected with a Climatronics All-In-One Weather Sensor (Part Number 102780), co-located with the gas measurements. Met data from throughout the project are shown in Fig. S1.

## 3. Results and discussion

### 3.1. Atmospheric concentrations: $NO_x$ and $NO_y$

A timeline of all gas measurements during GrandTReNDS is shown in Fig. 3. Measured $NO_x$ concentrations were generally low, with a median value of 0.54 ppb for the entire study, indicative of a remote site (Fahey et al., 1986; Hayden et al., 2003; Pandey Deolal et al., 2012). $NO_y$ concentrations had a median value of 1.32 ppb throughout the study, again typical for a rural sampling location (Hayden et al., 2003). A summary of measured concentrations from

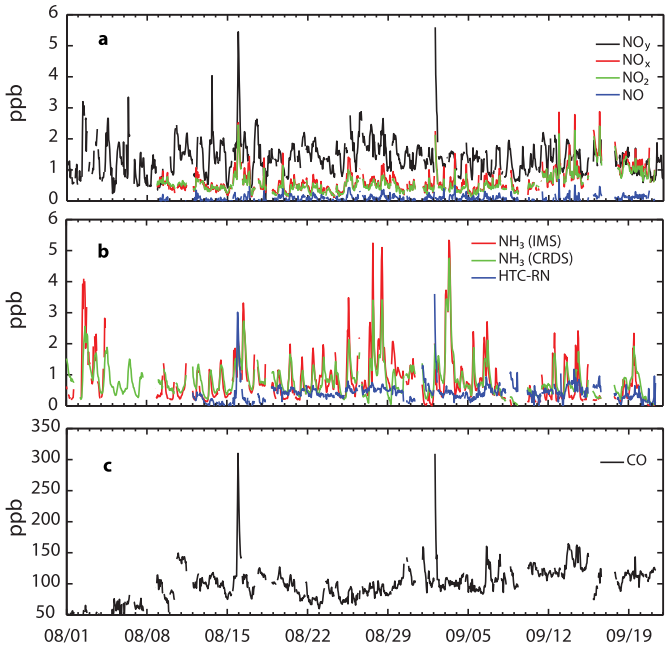


**Fig. 3.** One hour averaged concentrations for a) $NO_y$, $NO_x$, $NO_2$ and NO; b) $NH_3$ from the IMS and CRDS instruments and for HTC-RN; and c) CO.

throughout the campaign is given in Table 1. Although $NO_x$ and $NO_y$ concentrations were typically low, there are spikes in $NO_x$ and $NO_y$ on August 15–16 and September 2. These peaks are associated with biomass burning episodes and are discussed below. Also apparent in Fig. 3a is an increase in $NO_x$ relative to $NO_y$ beginning September 7 and continuing to the end of the study. Low values of $NO_x/NO_y$ are expected for remote areas (Fahey et al., 1986), with increasing conversion of $NO_x$ to $NO_y$ downwind of sources, particularly in summer (Hayden et al., 2003). Prior to September 7, $NO_x$ accounted for just 39% of $NO_y$; after the shift, $NO_x/NO_y$ increased to 76%, suggesting a source of $NO_x$ nearer to the site. During this period, HYSPLIT back-trajectories show that airmasses reaching the site had passed through areas in WY, ID and MT with active fires, as detected from MODIS. Carbon monoxide (Fig. 3c), particulate potassium and particulate organic carbon were also elevated during this time period (Fig. S2), all suggestive of regional biomass burning impacts.

Median hourly values for NO, $NO_2$, $NO_x$, $NO_y$ and $CN_{>40\ nm}$ for the entire study period are shown in Fig. 4. NO values had a broad daytime maximum that corresponded to increased temperatures, presumably due, in part, to $NO_2$ photolysis. $NO_2$ concentrations also showed a broad maximum, as did $NO_x$, $NO_y$ and $CN_{>40\ nm}$. The increase in all species is partially explained by the daily cycle in wind direction, also shown in Fig. 4. During summer, synoptic scale flows

**Table 1**
Summary trace gas and CN concentrations from GrandTReNDS.

| | Minimum (1 h) | Maximum (1 h) | Mean | Median |
|---|---|---|---|---|
| NO (ppb) | 0.0 | 0.7 | 0.07 | 0.06 |
| $NO_2$ (ppb) | 0.1 | 2.4 | 0.58 | 0.49 |
| $NO_x$ (ppb) | 0.1 | 2.9 | 0.66 | 0.54 |
| $NO_y$ (ppb) | 0.2 | 5.6 | 1.37 | 1.32 |
| $NH_3$ (IMS; ppb) | 0.0 | 5.3 | 0.79 | 0.56 |
| $NH_3$ (CRDS; ppb) | 0.0 | 4.8 | 0.83 | 0.70 |
| HTC-RN | 0.0 | 3.6 | 0.42 | 0.40 |
| CO (ppb) | 30 | 310 | 100 | 101 |
| CN ($cm^{-3}$) | 179 | 7346 | 1441 | 1329 |

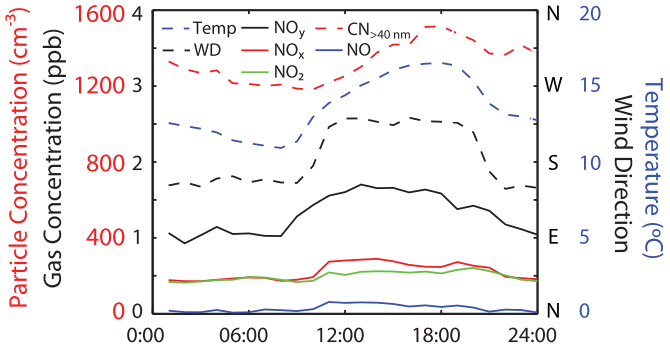


**Fig. 4.** Study median hourly values for NO, $NO_2$, $NO_x$, $NO_y$ and $CN_{>40\ nm}$. Also shown are project average temperature and wind direction at the core site. Met data were not available from 8/1–8/13 and 8/27–8/29.

in this region are typically weak, such that thermally driven winds frequently dominate circulation patterns (Stewart et al., 2002). For our sampling site, this equates to up-valley flows from the southwest during the day, and winds primarily from the southeast during the evening and early morning. The exact direction of the measured air flow was likely impacted by the complex topography at the site. In any case, to the east lies a pristine region with few sources (see inset in Fig. 1). Jackson, WY lies SE and further SE are large oil and gas fields near Pinedale, WY; however, our sampling site and Jackson were separated by the Teton Range, and so we were likely sheltered from any major impacts from these areas. In contrast, daytime southwesterly flow was likely impacted by emissions from Driggs, ~10 km away, as well as a series of towns further west (Fig. 1 inset). We calculated median $NO_x$ and $NO_y$ concentrations when 10 m surface winds were from the southwest (205°–245°) versus southeast (115°–155°); this includes cases in which the winds did not follow the pattern in Fig. 4. For this comparison, we removed observations impacted by biomass burning. We found that both $NO_x$ and $NO_y$ concentrations were higher when winds came from the SW versus the SE, by 21% and 29%, respectively. Although differences in concentrations for SW versus SE flow were statistically significant ($\alpha = 0.01$), suggesting an important role for the mountain-valley circulation, segregating by wind direction alone did not yield the magnitude of diel variability apparent in Fig. 4, where peak concentrations are ~50% greater than early morning values. For $NO_x$ and $NO_y$, variability in emissions likely also played a role, as did other potential factors, which are discussed below.

### 3.2. Atmospheric concentrations: $NH_3$ and HTC-RN

Concentrations of ammonia, measured from two instruments, and HTC-RN are shown in Fig. 3b. Average ammonia concentrations fall between those of $NO_x$ and $NO_y$ at 0.8 ppb. When considering individual species (e.g. $HNO_3$ instead of $NO_y$), ammonia was determined to be the most abundant gas phase reactive nitrogen species in the region during GrandTReNDS, based on these measurements and measurements made using an annular denuder system. This, coupled with its high deposition velocity, made $NH_3$ the dominant dry deposition reactive nitrogen species during GrandTReNDS (Benedict et al., 2013a). On several occasions, relatively high concentrations of ammonia were observed. Two of these events were related to biomass burning episodes and are described below, but two periods of elevated $NH_3$ (8/2–8/4 and 8/25–8/28) were not associated with biomass burning. During these periods, HYSPLIT back-trajectories suggest the airmasses came predominantly from Utah and the Snake River Valley, areas known to be important ammonia sources. HTC-RN also showed enhancements during biomass burning episodes, but maintained a relatively stable signal throughout much of the study, with a median concentration of 0.40 ppb. This value is comparable in magnitude to the detection limit of the Teledyne 201e instrument.

One goal of the study was to provide an intercomparison of the two ammonia instruments. Previous comparisons of multiple ammonia instruments, including a CRDS from Picarro and an IMS from Particle Measuring Systems, have shown overall good agreement (Schwab et al., 2007; von Bobrutzki et al., 2010), but with greater variability at concentrations <10 ppb (von Bobrutzki et al., 2010), which encompasses all of our measurements. A comparison of hourly concentrations throughout the campaign yielded $R^2 = 0.75$ between the two instruments, with the IMS having slightly higher values at high concentrations and the CRDS having slightly higher values at low concentrations (Fig. S3). Over the duration of the project, the two measurements had comparable average values (Table 1).

As was the case for the oxidized nitrogen species, a diel cycle was observed in ammonia concentrations (Fig. 5). Both instruments showed an increase in $NH_3$ each morning, peaking around noon, and then decaying throughout the remainder of the day. Higher emissions during the warmer daytime hours are expected to play a role in this cycle. Another factor likely impacting concentrations is the source of the air, with higher ammonia emissions expected southwest of the site during the day, and more pristine conditions to the east primarily at night. We again segregated average concentrations based on wind direction, and we removed all observations impacted by biomass burning. For $NH_3$, median concentrations were 43% higher when winds came from the SW versus the SE, and again this difference was statistically significant ($\alpha = 0.05$). However, concentration differences based on wind direction accounted for only a fraction of the differences observed mid-day compared to early morning. Previous studies have observed similar diel cycles in $NH_3$ concentrations in remote areas (Erisman et al., 2001; Olszyna et al., 2005). Saylor et al. (2010) put forth a possible mechanism to explain such an observed cycle. These authors suggest that in remote areas a shallow nocturnal boundary layer leads to dry deposition of $NH_3$, resulting in minimum concentrations near the surface at night. For our site, a collapsing boundary layer also drives air down slope, bringing cleaner air from higher elevations. During the day, valley air is driven upslope and air which is not depleted is mixed downward from aloft, leading to maximum concentrations around mid-day. Increasing temperature and decreasing RH can also lead to increased atmospheric $NH_3$ concentrations due to bi-directional exchange of ammonia between vegetation and the atmosphere

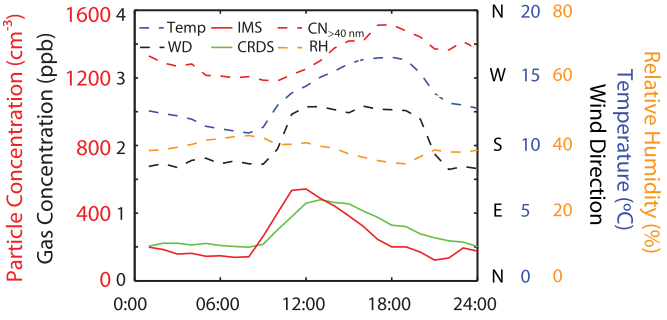


**Fig. 5.** Study median hourly ammonia concentrations from the CRDS and IMS instruments. Also shown are project average relative humidity, temperature and wind direction at the core site and median $CN_{>40\ nm}$ concentrations. Met data were not available from 8/1–8/13 and 8/27–8/29.

(Asman et al., 1998; Massad et al., 2010), and a shift in partitioning of ammonium nitrate particles, which favors the gas phase.

Although there are several real factors controlling ammonia concentrations, some of the observed variability may result from a sampling artifact, whereby ammonia adsorbs to surfaces in the inlet during the cold nighttime hours and is released when the sun warms the inlet. Particulate $NH_4NO_3$ may also be trapped in the inlet filter and volatilized when heated. However, mean ammonium nitrate concentrations were only 0.15 μg $m^{-3}$, and so any volatilized $NH_4NO_3$ would not likely dominate the ammonia signal. To test for artifacts, for select periods we collected concurrent samples using URG annular denuders. The URG samplers, which first collect gases by diffusion upstream and particles on a downstream filter, are not expected to suffer from these same artifacts. Sampling times with the URG samplers were varied (3–20 h) and covered different times of the day, in an attempt to capture the variability in the observed concentrations. Extracted samples were analyzed by ion chromatography (Benedict et al., 2013a). Data collected with URG samplers are compared to both the IMS and the CRDS in Fig. 6; sampling duration for the denuders is also included. The reasonably good agreement between the real-time instruments and the URG samplers ($R^2_{URG\text{-}ASII} = 0.61$; $R^2_{URG\text{-}Pic} = 0.50$) validates the measured diel cycle. Nevertheless, there is scatter for both instruments when compared to the denuder. Many outliers were observed during the shortest sampling times, and all of the shortest sampling periods occurred between the hours of 5–9 AM, when losses in the inlet may occur. Of the remaining data, the light blue points were typically collected from 6 AM to 2 PM, during peak ammonia concentrations; these data are scattered about the 1:1 line. The orange points typically were collected from 2 PM to 6 AM; the real time data appear to be biased low during these periods, suggestive of losses in the inlet at these times. Data collected during the biomass burning events are discussed below.

### 3.3. Biomass burning episodes

Two of the high ammonia concentrations apparent in Fig. 3b, August 15–16 and September 2, occurred when the site was exposed to elevated levels of biomass burning emissions. Data are shown for both of these events in Fig. 7. In both cases, carbon monoxide is used as an indicator for the presence of smoke, with concentrations increasing from ~100 ppb to ~300 ppb in the late evening on August 15 and early morning on September 2. Total particle number (Fig. S4), particulate organics and particle-phase potassium ion concentrations (Fig. S2) were also elevated during this time. With the smoke, $NO_x$ and $NO_y$ concentrations increased, as did $NH_3$ and HTC-RN concentrations. Interestingly, in both cases the ammonia showed a second peak, hours later. The secondary peaks could be influenced by adsorption of ammonia in the inlet during the nighttime smoke events, followed by desorption during the hotter daytime hours. The data from August 15–16 are consistent with such a mechanism, with the largest concentrations observed at noon on August 16. By again comparing to the denuder data we find the denuder measurements were greater than those measured by the CRDS by 0.7 ppb during the smoke period, while the denuder measurements were lower than the measured ammonia from the CRDS by 0.4 ppb after the smoke event, indicative of inlet effects. Another possible factor for the daytime increase is bi-directional exchange of the ammonia associated with the smoke with the underlying vegetation, resulting in a delay in transport of the ammonia. There was also a change in wind direction coincident with the increase, potentially bringing $NH_3$ from other sources. The data from September 2 also show a small increase in ammonia during the daytime hours following the smoke event, which may have been impacted by inlet effects and bi-directional exchange. However, much larger peaks are evident starting early on September 3, when desorption from the inlet is not expected. The increasing ammonia occurs shortly after winds shift from SW to SE. This large, post-smoke event peak thus appears to be driven more by a change in air mass than any inlet effect and may include sources unrelated to the biomass burning episode.

In addition to the high concentrations of the known nitrogen species, the two smoke events provided the only elevated concentrations in the HTC-RN measurement. Biomass burning plumes are also expected to have high VOC concentrations, and chemiluminescence instruments are known to respond to certain organics species which do not contain nitrogen (Grosjean and Harrison, 1985). Using our measured CO concentrations, we estimate a maximum VOC concentration of 27 ppb based on emission factors from fires for a temperate evergreen needleleaf forest ((Wiedinmyer et al., 2011), with updated values from http://bai.acd.ucar.edu/Data/fire/). Given that only certain VOCs cause a positive interference using chemiluminescence, and of these the interference is typically less than 1% of the VOC concentration for chemiluminescence techniques using a lower temperature molybdenum converter (Bloss et al., 2012), interference from VOCs does not appear to account for all of the HTC-RN signal, and so other nitrogen compounds are presumed to be present in the sample. Although these compounds were not speciated, other nitrogen containing compounds that have previously been identified in biomass burning emissions include hydrogen cyanide (Yokelson et al., 1996), nitriles (Andreae and Merlet, 2001; Yokelson et al., 1996), and isocyanic acid (Roberts et al., 2011). Amines also may have been present, but were removed along with ammonia in the

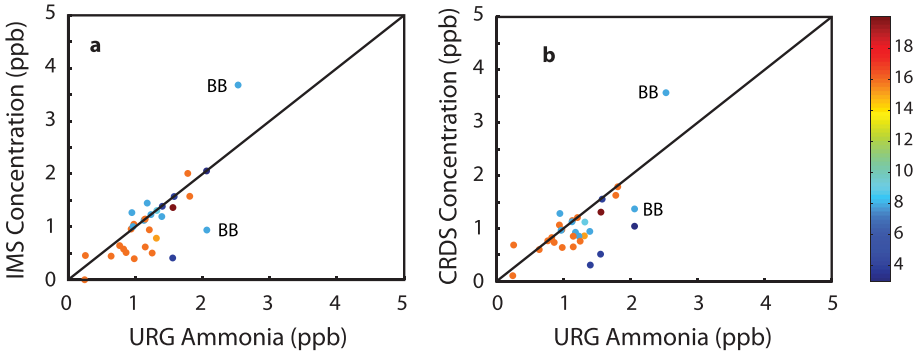


**Fig. 6.** a) Comparison of IMS results with concurrent denuder measurements. b) Comparison of CRDS results with the same denuder measurements. A one-to-one line is shown for comparison. Data points are color-coded based on the number of hours sampled. BB designates samples that were collected during or immediately after the biomass burning episode on September 2.

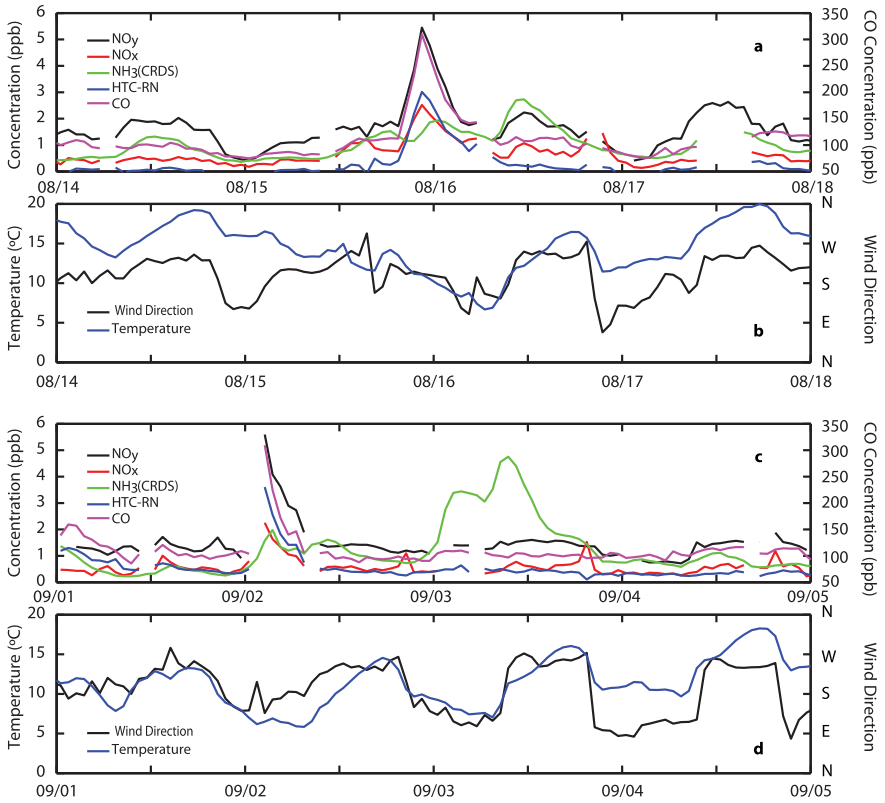


**Fig. 7.** Measured concentrations and meteorological data during biomass burning episodes on (a, b) August 15–16 and (c, d) September 2.

upstream denuder. In addition to HTC-RN in the gas phase, enhanced concentrations of particulate organic nitrogen were also detected with an Aerosol Mass Spectrometer (not shown) and in the filter samples during the biomass burning events. These data support previous measurements which suggest that biomass burning provides a potentially large natural source of atmospheric nitrogen (Wiedinmyer et al., 2011; Yokelson et al., 1996).

## 4. Conclusions

High time resolution measurements of atmospheric reactive nitrogen species were collected for two months during GrandTReNDS. For the entire study, the average $NO_y$ concentration was 1.37 ppb (median = 1.32 ppb), the average $NO_x$ concentration was 0.66 ppb (median = 0.54 ppb), and the average ammonia concentration was 0.8 ppb (IMS median 0.56 ppb; CRDS median = 0.70 ppb). Reactive nitrogen concentrations at the site were partly driven by thermally influenced circulations, with concentrations of all measured species peaking during the day when air was transported to the site from the valley below. Reactive nitrogen concentrations further east in GRTE are less likely to be impacted by upslope winds from the west, and indeed measurements collected throughout GRTE show a gradient in ammonia concentration which decreases from west to east (Benedict et al., 2013a). While it appears that mountain valley circulations partially drove the diel cycle of concentrations, changing boundary layer heights and mixing from aloft likely also played a role in the observed cycles. Using trajectory analysis, Benedict et al. (2013a) have shown that air mass history also impacted concentrations, with enhanced ammonia concentrations observed when air masses passed through the Snake River Valley and northern Utah and during periods of stagnation. In addition to local sources and long range transport, biomass burning was identified as an important intermittent source of reactive nitrogen to this region.

## Acknowledgments

This project was funded by the NPS (P11AT70958 and H2370094000). The authors wish to thank the staffs at Grand Targhee Resort, GRTE, and the USFS Teton Basin Ranger District for site access and logistical support. The authors wish to thank Jim Robertson for providing details regarding vegetation at the site and Drew Bingham for assisting with creating the map inset in Fig. 1. The authors would especially like to acknowledge Rick Swanker at Grand Targhee for his help in many phases of the project. The assumptions, findings, conclusions, judgments, and views presented herein are those of the authors and should not be interpreted as necessarily representing the NPS. We acknowledge the use of FIRMS data from the Land Atmosphere Near-real time Capability for EOS (LANCE) system operated by the NASA/GSFC/Earth Science Data and Information System (ESDIS) with funding provided by NASA/HQ.

## Appendix A. Supplementary data

Supplementary data related to this article can be found at http://dx.doi.org/10.1016/j.atmosenv.2014.03.017.

## References

Alkezweeny, A.J., Laws, G.L., Jones, W., 1986. Aircraft and ground measurements of ammonia in Kentucky. Atmospheric Environment 20, 357–360.
Andreae, M.O., Merlet, P., 2001. Emission of trace gases and aerosols from biomass burning. Global Biogeochemical Cycles 15, 955–966.
Asman, W.A.H., Sutton, M.A., Schjorring, J.K., 1998. Ammonia: emission, atmospheric transport and deposition. New Phytologist 139, 27–48.

Beem, K.B., Raja, S., Schwandner, F.M., Taylor, C., Lee, T., Sullivan, A.P., Carrico, C.M., McMeeking, G.R., Day, D., Levin, E., Hand, J., Kreidenweis, S.M., Schichtel, B., Malm, W.C., Collett, J.L., 2010. Deposition of reactive nitrogen during the Rocky Mountain Airborne Nitrogen and Sulfur (RoMANS) study. Environmental Pollution 158, 862–872.

Benedict, K.B., Chen, X., Sullivan, A.P., Li, Y., Day, D., Prenni, A.J., Levin, E.J.T., Kreidenweis, S.M., Malm, W.C., Schichtel Jr., B.A., Collett Jr., Jeffrey L., 2013a. Atmospheric concentrations and deposition of reactive nitrogen in Grand Teton National Park. Journal of Geophysical Research: Atmospheres 118. http://dx.doi.org/10.1002/2013JD020394.

Benedict, K.B., Carrico, C.M., Kreidenweis, S.M., Schichtel, B., Malm, W.C., Collett, J.L., 2013b. A seasonal nitrogen deposition budget for Rocky Mountain National Park. Ecological Applications 23, 1156–1169.

Birch, M.E., Cary, R.A., 1996. Elemental carbon-based method for monitoring occupational exposures to particulate diesel exhaust. Aerosol Science and Technology 25, 221–241.

Bloss, W.J., Alam, M.S., Lee, J.D., Vázquez, M., Munoz, A., Ródenas, M., 2012. NOx Analyser Interference from Alkenes. European Geophysical Union General Assembly, Vienna, Austria. Geophys. Res. Abstr. 14, EGU2012–6330.

Bowman, W.D., Gartner, J.R., Holland, K., Wiedermann, M., 2006. Nitrogen critical loads for alpine vegetation and terrestrial ecosystem response: are we there yet? Ecological Applications 16, 1183–1193.

Bowman, W.D., Theodose, T.A., Schardt, J.C., Conant, R.T., 1993. Constraints of nutrient availability on primary production in 2 alpine tundra communities. Ecology 74, 2085–2097.

Burns, D.A., 2003. Atmospheric nitrogen deposition in the Rocky Mountains of Colorado and southern Wyoming – a review and new analysis of past study results. Atmospheric Environment 37, 921–932.

Clarisse, L., Clerbaux, C., Dentener, F., Hurtmans, D., Coheur, P.F., 2009. Global ammonia distribution derived from infrared satellite observations. Nature Geoscience 2, 479–483.

Day, D.E., Chen, X., Gebhart, K.A., Carrico, C.M., Schwandner, F.M., Benedict, K.B., Schichtel, B.A., Collett, J.L., 2012. Spatial and temporal variability of ammonia and other inorganic aerosol species. Atmospheric Environment 61, 490–498.

Draxler, R.R., 1999. HYSPLIT4 User's Guide. NOAA Air Resources Laboratory, Silver Spring, MD.

Draxler, R.R., Hess, G.D., 1998. An overview of the HYSPLIT_4 modeling system of trajectories, dispersion, and deposition. Australian Meteorological Magazine 47, 295–308.

Dunlea, E.J., Herndon, S.C., Nelson, D.D., Volkamer, R.M., San Martini, F., Sheehy, P.M., Zahniser, M.S., Shorter, J.H., Wormhoudt, J.C., Lamb, B.K., Allwine, E.J., Gaffney, J.S., Marley, N.A., Grutter, M., Marquez, C., Blanco, S., Cardenas, B., Retama, A., Villegas, C.R.R., Kolb, C.E., Molina, L.T., Molina, M.J., 2007. Evaluation of nitrogen dioxide chemiluminescence monitors in a polluted urban environment. Atmospheric Chemistry and Physics 7, 2691–2704.

Erisman, J.W., Otjes, R., Hensen, A., Jongejan, P., van den Bulk, P., Khlystov, A., Mols, H., Slanina, S., 2001. Instrument development and application in studies and monitoring of ambient ammonia. Atmospheric Environment 35, 1913–1922.

Fahey, D.W., Hubler, G., Parrish, D.D., Williams, E.J., Norton, R.B., Ridley, B.A., Singh, H.B., Liu, S.C., Fehsenfeld, F.C., 1986. Reactive nitrogen species in the troposphere – measurements of NO, $NO_2$, $HNO_3$, particulate nitrate, peroxyacetyl nitrate (PAN), $O_3$, and total reactive odd nitrogen (NOy) at Niwot Ridge, Colorado. Journal of Geophysical Research: Atmospheres 91, 9781–9793.

Fehsenfeld, F.C., Dickerson, R.R., Hubler, G., Luke, W.T., Nunnermacker, L.J., Williams, E.J., Roberts, J.M., Calvert, J.G., Curran, C.M., Delany, A.C., Eubank, C.S., Fahey, D.W., Fried, A., Gandrud, B.W., Langford, A.O., Murphy, P.C., Norton, R.B., Pickering, K.E., Ridley, B.A., 1987. A ground-based intercomparison of NO, NOx, and NOy measurement techniques. Journal of Geophysical Research: Atmospheres 92, 14710–14722.

Fenn, M.E., Baron, J.S., Allen, E.B., Rueth, H.M., Nydick, K.R., Geiser, L., Bowman, W.D., Sickman, J.O., Meixner, T., Johnson, D.W., Neitlich, P., 2003a. Ecological effects of nitrogen deposition in the western United States. Bioscience 53, 404–420.

Fenn, M.E., Haeuber, R., Tonnesen, G.S., Baron, J.S., Grossman-Clarke, S., Hope, D., Jaffe, D.A., Copeland, S., Geiser, L., Rueth, H.M., Sickman, J.O., 2003b. Nitrogen emissions, deposition, and monitoring in the western United States. Bioscience 53, 391–403.

Fontijn, A., Sabadell, A.J., Ronco, R.J., 1970. Homogeneous chemiluminescent measurement of nitric oxide with ozone – implications for continuous selective monitoring of gaseous pollutants. Analytical Chemistry 42, 575–579.

Galloway, J.N., Dentener, F.J., Capone, D.G., Boyer, E.W., Howarth, R.W., Seitzinger, S.P., Asner, G.P., Cleveland, C.C., Green, P.A., Holland, E.A., Karl, D.M., Michaels, A.F., Porter, J.H., Townsend, A.R., Vorosmarty, C.J., 2004. Nitrogen cycles: past, present, and future. Biogeochemistry 70, 153–226.

Grosjean, D., Harrison, J., 1985. Response of chemiluminescence NOx analyzers and ultraviolet ozone analyzers to organic air pollutants. Environmental Science & Technology 19, 862–865.

Hand, J.L., Kreidenweis, S.M., 2002. A new method for retrieving particle refractive index and effective density from aerosol size distribution data. Aerosol Science and Technology 36, 1012–1026.

Hayden, K.L., Anlauf, K.G., Hastie, D.R., Bottenheim, J.W., 2003. Partitioning of reactive atmospheric nitrogen oxides at an elevated site in southern Quebec, Canada. Journal of Geophysical Research: Atmospheres 108.

Hill, H.H., Siems, W.F., Stlouis, R.H., McMinn, D.G., 1990. Ion mobility spectrometry. Analytical Chemistry 62, A1201–A1209.

Holtgrieve, G.W., Schindler, D.E., Hobbs, W.O., Leavitt, P.R., Ward, E.J., Bunting, L., Chen, G.J., Finney, B.P., Gregory-Eaves, I., Holmgren, S., Lisac, M.J., Lisi, P.J., Nydick, K., Rogers, L.A., Saros, J.E., Selbie, D.T., Shapley, M.D., Walsh, P.B., Wolfe, A.P., 2011. A coherent signature of anthropogenic nitrogen deposition to remote watersheds of the northern hemisphere. Science 334, 1545–1548.

Kallinger, G., Niessner, R., 1999. Laboratory investigation of annular denuders as sampling system for the determination of aliphatic primary and secondary amines in stack gas. Mikrochimica Acta 130, 309–316.

Kopacek, J., Posch, M., 2011. Anthropogenic nitrogen emissions during the Holocene and their possible effects on remote ecosystems. Global Biogeochemical Cycles 25. http://dx.doi.org/10.1029/2010gb003779.

Krupa, S.V., 2003. Effects of atmospheric ammonia ($NH_3$) on terrestrial vegetation: a review. Environmental Pollution 124, 179–221.

Marx, O., Brümmer, C., Ammann, C., Wolff, V., Freibauer, A., 2012. TRANC – a novel fast-response converter to measure total reactive atmospheric nitrogen. Atmospheric Measurement Techniques 5, 1045–1057.

Massad, R.S., Nemitz, E., Sutton, M.A., 2010. Review and parameterisation of bi-directional ammonia exchange between vegetation and the atmosphere. Atmospheric Chemistry and Physics 10, 10359–10386.

Nanus, L., Williams, M.W., Campbell, D.H., Tonnessen, K.A., Blett, T., Clow, D.W., 2009. Assessment of lake sensitivity to acidic deposition in national parks of the Rocky Mountains. Ecological Applications 19, 961–973.

Olszyna, K.J., Bairai, S.T., Tanner, R.L., 2005. Effect of ambient $NH_3$ levels on PM2.5 composition in the Great Smoky Mountains National Park. Atmospheric Environment 39, 4593–4606.

Paldus, B.A., Kachanov, A.A., 2005. An historical overview of cavity-enhanced methods. Canadian Journal of Physics 83, 975–999.

Pandey Deolal, S., Brunner, D., Steinbacher, M., Weers, U., Staehelin, J., 2012. Long-term in situ measurements of NOx and NOy at Jungfraujoch 1998-2009: time series analysis and evaluation. Atmospheric Chemistry and Physics 12, 2551–2566.

Parrish, D.D., Fehsenfeld, F.C., 2000. Methods for gas-phase measurements of ozone, ozone precursors and aerosol precursors. Atmospheric Environment 34, 1921–1957.

Reis, S., Pinder, R.W., Zhang, M., Lijie, G., Sutton, M.A., 2009. Reactive nitrogen in atmospheric emission inventories. Atmospheric Chemistry and Physics 9, 7657–7677.

Roberts, J.M., Veres, P.R., Cochran, A.K., Warneke, C., Burling, I.R., Yokelson, R.J., Lerner, B., Gilman, J.B., Kuster, W.C., Fall, R., de Gouw, J., 2011. Isocyanic acid in the atmosphere and its possible link to smoke-related health effects. Proceedings of the National Academy of Sciences of the United States of America 108, 8966–8971.

Saros, J.E., Clow, D.W., Blett, T., Wolfe, A.P., 2011. Critical nitrogen deposition loads in high-elevation lakes of the Western US inferred from paleolimnological records. Water Air and Soil Pollution 216, 193–202.

Saylor, R.D., Edgerton, E.S., Hartsell, B.E., Baumann, K., Hansen, D.A., 2010. Continuous gaseous and total ammonia measurements from the southeastern aerosol research and characterization (SEARCH) study. Atmospheric Environment 44, 4994–5004.

Schwab, J.J., Li, Y.Q., Bae, M.S., Demerjian, K.L., Hou, J., Zhou, X.L., Jensen, B., Pryor, S.C., 2007. A laboratory intercomparison of real-time gaseous ammonia measurement methods. Environmental Science & Technology 41, 8412–8419.

Seinfeld, J.H., Pandis, S.N., 1998. Atmospheric Chemistry and Physics: from Air Pollution to Climate Change. John Wiley and Sons, Inc., New York.

Sheppard, L.J., Leith, I.D., Mizunuma, T., Cape, J.N., Crossley, A., Leeson, S., Sutton, M.A., van Dijk, N., Fowler, D., 2011. Dry deposition of ammonia gas drives species change faster than wet deposition of ammonium ions: evidence from a long-term field manipulation. Global Change Biology 17, 3589–3607.

Sintermann, J., Ammann, C., Kuhn, U., Spirig, C., Hirschberger, R., Gartner, A., Neftel, A., 2011. Determination of field scale ammonia emissions for common slurry spreading practice with two independent methods. Atmospheric Measurement Techniques 4, 1821–1840.

Stewart, J.Q., Whiteman, C.D., Steenburgh, W.J., Bian, X.D., 2002. A climatological study of thermally driven wind systems of the US Intermountain West. Bulletin of the American Meteorological Society 83, 699–708.

Sullivan, A.P., Frank, N., Onstad, G., Simpson, C.D., Collett, J.L., 2011. Application of high-performance anion-exchange chromatography-pulsed amperometric detection for measuring carbohydrates in routine daily filter samples collected by a national network: 1. Determination of the impact of biomass burning in the upper Midwest. Journal of Geophysical Research: Atmospheres 116. http://dx.doi.org/10.1029/2010JD014166.

von Bobrutzki, K., Braban, C.F., Famulari, D., Jones, S.K., Blackall, T., Smith, T.E.L., Blom, M., Coe, H., Gallagher, M., Ghalaieny, M., McGillen, M.R., Percival, C.J., Whitehead, J.D., Ellis, R., Murphy, J., Mohacsi, A., Pogany, A., Junninen, H., Rantanen, S., Sutton, M.A., Nemitz, E., 2010. Field inter-comparison of eleven atmospheric ammonia measurement techniques. Atmospheric Measurement Techniques 3, 91–112.

Wiedinmyer, C., Akagi, S.K., Yokelson, R.J., Emmons, L.K., Al-Saadi, J.A., Orlando, J.J., Soja, A.J., 2011. The Fire INventory from NCAR (FINN): a high resolution global model to estimate the emissions from open burning. Geoscientific Model Development 4, 625–641.

Williams, M.W., Baron, J.S., Caine, N., Sommerfeld, R., Sanford, R., 1996. Nitrogen saturation in the Rocky Mountains. Environmental Science & Technology 30, 640–646.

Yokelson, R.J., Griffith, D.W.T., Ward, D.E., 1996. Open-path Fourier transform infrared studies of large-scale laboratory biomass fires. Journal of Geophysical Research: Atmospheres 101, 21067–21080.